CMLS, Cell. Mol. Life Sci. 54 (1998) 476–487
1420-682X/98/050476-12 $ 1.50 + 0.20/0

CMLS Cellular and Molecular Life Sciences

Research Article

Dictyostelium discoideum cells shed vesicles with associated DNA and vital stain Hoechst 33342

I. Tatischeff[a,*], M. Bomsel[b], C. de Paillerets[c], H. Durand[b], B. Geny[b], D. Segretain[d], E. Turpin[b] and A. Alfsen[c]

[a]Laboratoire de Physicochimie Biomoléculaire et Cellulaire, CNRS URA 2056, Université Pierre et Marie Curie, 4, Place Jussieu, Case 138, F-75252 Paris Cedex 05 (France), e-mail: tati@lpbc.jussieu.fr
[b]Signalisation, Inflammation et Transformation Cellulaire, U. 332, Institut Cochin de Génétique Moléculaire, 22, rue Méchain, F-75014 Paris (France)
[c]Etats Liés Moléculaires, Université René Descartes, 45, rue des Saints-Pères, F-75270 Paris Cedex 06 (France)
[d]Laboratoire d'Histologie et Embryologie, CHU Paris-Ouest, Faculté de Médecine, 45, rue des Saints-Pères, F-75270 Paris Cedex 06 (France)

Received 14 November 1997; received after revision 16 March 1998; accepted 16 March 1998

Abstract. *Dictyostelium discoideum* cells are highly resistant to xenobiotics. We previously observed that these primitive eukaryotic cells contain a 170-kDa P-glycoprotein, mediating multidrug resistance in mammalian cells, but nonfunctional in *Dictyostelium* cells. We show here that *D. discoideum* cells vitally stained with the DNA-specific dye, Hoechst 33342, release fluorescent material in their culture medium. Electron microscopy and lipid analysis demonstrate the vesicular nature of this material. Moreover, nucleic acids associate with these extracellular vesicles independently of Hoechst vital staining. The main vesicular DNA component exhibits a size >21 kb. Shedding of microvesicles during cell growth is not concomitant with programmed cell death. We propose that these extracellular vesicles are involved in a new cellular resistance mechanism against xenobiotics. Furthermore, since the association of DNA with vesicles occurs in physiological growth conditions and independently of vital staining, the new shedding process might be involved in a more general intercellular mechanism.

Key words. Multidrug resistance; extracellular vesicles; Hoechst 33342; DNA; *Dictyostelium discoideum*.

Dictyostelium discoideum cells are highly resistant to structurally unrelated xenobiotics such as the carcinogenic hydrocarbon benzo(a)pyrene [B(a)P] [1], the antitumoral antibiotic daunorubicin (DAU), DNA vital stains Dapi and Hoechst 33342 (HO342), mitochondrial vital stains Rhodamine 123 (Rh123) [2] and a carbocyanine dye JC-1. All these xenobiotics except Dapi are known substrates of the so-called P-glycoprotein (P-gp), a 170-kDa protein that mediates classical multidrug resistance (reviewed in refs 3–5).

* Corresponding author.

We have previously demonstrated biochemically the presence of a constitutive P-gp in *D. discoideum* cells by Western blot analysis with the anti-P-gp monoclonal antibody (mAb) JSB-1 [6] and, more recently, by flow cytometry analysis using two other anti-P-gp mAbs, C219 and MRK-16. Furthermore, hybridization of complementary DNA (cDNA), prepared from *D. discoideum* cell RNA and polymerase chain reaction (PCR)-amplified, with a human multidrug *MDR1* gene probe confirmed the presence of P-gp in *D. discoideum* cells (unpublished results). Despite the presence of a constitutive 170-kDa P-gp expressed by an *MDR1*-like

gene, the classical multidrug resistance mediated by this P-gp appeared nonfunctional, or the reversion process functions differently from the usual mechanism in *D. discoideum* cells [2].

Searching for a new resistance mechanism to explain the high endogeneous resistance of *D. discoideum* cells, we observed that, when cells were vitally stained with the DNA-targeted fluorescent HO342, a fluorescent material was released in the culture medium. The spectral characteristics of the fluorescence allowed us to identify HO342 as the emitting compound. After concentration, the vesicular nature of this fluorescent extracellular material was revealed by electron microscopy (EM) and lipid analysis. The new extracellular organelles were biochemically characterized by protein analysis and phospholipid identification. Nucleic acids were also found to be associated with these vesicles. A major vesicle DNA component exhibited a size >21 kb. Importantly, production of the extracellular organelles as well as presence of associated DNA did not rely on HO342 vital staining of the cells.

Materials and methods

Culture conditions. *D. discoideum* (*Dd*) cells, cloned Ax-2 strain [7], were grown in suspension in HL5 semi-defined medium [8], containing 7 g/l of yeast extract (Oxoid, Unipath, Dardilly, France), on a gyratory shaker (175 rpm) at 22 °C. For proper oxygenation, each suspension was grown in an Erlenmeyer containing five times the suspension volume. Cells are able to grow and divide at the expense of soluble or particulate nutrients to produce vegetative cells. Cells were generally used in the exponential growth phase. Cell viability was controlled either by trypan blue (0.05% w/v) or propidium iodide exclusion (2 µg/ml final concentration).

Vital staining of *D. discoideum* cells by HO342. Vital staining of *Dd* cells was performed in HL5 medium. The cellular density and the morphological appearance of the cells were controlled on a hemocytometer before and after HO342 vital staining. In the case of preparation of extracellular vesicles from vitally stained cells, HO342 (3 µg/ml) was added to a cell suspension at an initial density of 2×10^6 cells/ml. Cells were grown for 23 h in the continuous presence of HO342, reaching a still exponential density of 7×10^6 cells/ml. In the case of spectrophotometric studies, cells were incubated with indicated concentration of HO342 either for 0.5 to 5 h, a short incubation time relative to the mean generation time of amoebae (11 h), or for 72 h in long-term experiments. In order to eliminate extracellular HO342, cells were harvested by centrifugation at 700*g* for 5 min, washed twice in ice-cold buffer A [17 mM potassium phosphate (pH 6.8)] and resuspended in the same buffer at a density of 2×10^7 cells/ml.

Light microscopy of *D. discoideum* cells and extracellular material. After vital staining, cells were either kept alive at 4 °C until observation by light microscopy or fixed at 2×10^7 cells/ml in methanol:buffer A (70:30 v/v), which improved nuclear access to the previously intracellularly accumulated HO342. Alternatively, cells fixed after vital staining were further prepared for long-term conservation on glass slides as follows. Ten-microlitre deposits of the fixed cell suspension were allowed to air-dry on methanol-washed slides before addition of 25 µl of pure methanol that was further air-dried. After mounting in 15 µl of glycerol:buffer A (20:80 v/v), slides were kept at 4 °C and remained observable for several weeks.

Phase contrast and ultraviolet (UV) fluorescence microscopy were performed with a BHA Olympus microscope (Scop, Rungis, France), equipped with a 100-W mercury lamp and a UV-blue fluorescence excitation block. Pictures were taken with either Kodak Ektachrome Professional P800/1600 film or FUJI 400 ASA film for color slides.

Preparation of *D. discoideum* extracellular material. Extracellular material was prepared from at most 400 ml of culture medium from *Dd* cells. Cells grown with or without vital staining were centrifuged at 700*g* for 5 min, and cell-free supernatant was centrifuged at 105,000*g* for 1 h, using a refrigerated L5-50DB Beckman centrifuge with a Ti 60 rotor. Clarified supernatant was discarded, after an aliquot had been kept for protein concentration measurement. The pellet was resuspended in 1/100 of initial volume with buffer B [10 mM Tris (pH 7.05)] and kept at 4 °C. This extracellular material was analysed by a density gradient as previously described for intracellular clathrin-coated vesicles [9]. Briefly, 1 ml was diluted twice in buffer B and layered on top of the D_2O-sucrose step gradient between 1.050 and 1.210 g/cm^3 density. After centrifugation at 4 °C in an SW28 rotor at 90,000*g* for 2 h, the pellet and five fractions were collected and extensively dialysed overnight at 4 °C against buffer B. Samples were stored at 4 °C.

HL5 medium alone was treated in the same way as the 700*g* cell-free supernatant. The 105,000*g* pellet was suspended in 1/100 of initial volume with buffer B and used as a control for further protein, lipid and nucleic acid analyses.

EM of *D. discoideum* extracellular material. *Dd* concentrated extracellular material has been observed by a negative staining technique. The material was washed after fixation in 2.5% (v/v) glutaraldehyde, deposited on a formvar (2%)-coated grid, stained with phosphotungstic acid (2% in water) and air-dried. Samples were

observed at 60 kV with a Philips CM 10 electron microscope (Institut Alfred Feyssard, CNRS, Gif-sur-Yvette).

Protein analyses. Protein concentrations were determined according to Peterson [10]. Polypeptide components were analysed by SDS-polyacrylamide gel electrophoresis (PAGE) under reducing conditions [11].

Lipid analyses from *D. discoideum* extracellular material. Lipids were extracted in chloroform/methanol at room temperature [12]. One ml of concentrated *Dd* extracellular material was extracted twice with 30 ml of chloroform:methanol (2:1 v/v) (CM) and addition of 1 ml of distilled water. After evaporation of the organic phase, lipids were resuspended in 2 ml of CM and stored under N_2 at 4 °C. For thin-layer chromatography (TLC), 250-µl samples of extracted lipids were dried under N_2 at 4 °C and resuspended in 50 µl of chloroform. For one-dimensional TLC, lipids were spotted on silica plates and separated in chloroform:methanol:acetic acid:water (75:45:12:2 v/v/v/v). Membrane lipids extracted from HL60 cells [13] were used as standards. Phospholipids, i.e. phosphatidic acid (PA), phosphatidylethanolamine (PE), phosphatidylinositol (PI), phosphatidylserine (PS), phosphatidylcholine (PC) and sphingomyelin (Sph), were visualized by transient staining with iodine vapour. Two-dimensional TLC separation was performed according to Rouser et al. [14]. In addition to iodine vapour staining, ninhydrin staining was used to further characterize the amino group-containing phospholipids (PE and PS).

Nucleic acid analyses from *D. discoideum* extracellular material. Extraction of all nucleic acids (DNA and RNA) from *Dd* extracellular material was performed according to a commonly used technique in molecular biology [15]. Briefly, nucleic acids were extracted at a microscale, as follows. Concentrated *Dd* extracellular material (150–600 µl) was mixed by hand shaking in the same volume of phenol:chloroform:isoamylic alcohol (25:24:1 v/v/v). Using this mixture [15] allows inactivation of RNase and efficient deproteinization, which was confirmed with a further control of protein digestion by addition of proteinase K to the nucleic acid sample. Nucleic acid purification was carried out by centrifugation at 15,000*g* for 5 min. The upper aqueous phase inholding nucleic acids were transferred to a fresh tube. The organic phase and interface were reextracted at least once, and the aqueous phases were pooled. Nucleic acids, contained in the total aqueous phase, were precipitated at −80 °C for 30 min with 2 vol of glacial ethanol in the presence of 0.25 M NaCl. Then the pellet was recovered by centrifugation at 17,000*g* for 30 min, followed by a 5-min wash in 70% ethanol, and dried free of ethanol before storage at −20 °C. For nucleic acid analysis by electrophoresis, each dry sample was suspended in 20 µl of sample buffer (10 mM Tris, 1 mM EDTA). Ten µl were layered on 1% agarose gels, containing ethidium bromide (0.6 µg/ml). Electrophoreses were run at 120 V, for about 30 min, in a minisubcell (BioRad, Ivry, France) and revealed by using UV excitation of nucleic acid-bound ethidium bromide. To distinguish between RNA and DNA, nucleic acids were pretreated, before electrophoresis, for 1 h at 37 °C, with either DNase (Promega, Madison, WI, USA) (1 or 4 U/ml) or with RNase (DNase-free, Boerhinger Manheim France, Meylan) (1 µg/ml).

Spectrofluorimetric measurements. Spectrofluorimetric measurements were performed with an HP 9835 computer-automated setup, specially equipped for the study of whole cells and membranes [16]. The intensity of the monochromatic excitation light was monitored with a Rhodamine B quantum counter (3 g/l in ethylene glycol) in order to correct the emission and excitation spectra for fluctuation in excitation light intensity. Spectra were not corrected for instrumental response, since only relative variations of the fluorescence parameters were analysed.

For determination of HO342 incorporation into *Dd* cells, the cellular suspension was diluted to 5×10^6 cells/ml in buffer A, prior to fluorescence measurements in a 2×10-mm quartz cuvette. This procedure avoided diffusion artefacts observed at high cell density and the 280-nm excited fluorescence remained in the linear portion of protein fluorescence.

Results

Analysis by light microscopy after HO342 vital staining of *D. discoideum* cells. Important differences in fluorescent staining were observed between live cells and cells post-fixed after vital staining with HO342. Nuclei of *Dd* live cells were not immediately visible after incubation of the cells for 0.5 h with HO342 at a concentration of 12 µg/ml for vital staining. As shown in figure 1A, cells rounded up with blebbing and increased vacuolization after an additional incubation for 7 h at 4 °C. In spite of these morphological stress signals, cells were still alive as measured by trypan blue or propidium iodide exclusion. Under these conditions, nuclei remained poorly accessible to HO342, and a faint punctuated cytoplasmic fluorescence pattern was visible (fig. 1B). After 10 more minutes of oxygen stress under coverglass, the fluorescence intensity of the already labelled nuclei increased, and additional nuclei appeared labelled (fig. 1D). The punctuated label seemed to increase especially in the cytoplasm of cells that had lost their blebs (fig. 1C, arrows). In contrast with the above observations on live cells, cells vitally stained with HO342 but immediately post-fixed in 70% methanol exhibited a strong and homogeneous nuclei fluorescence (fig. 1E). As a control

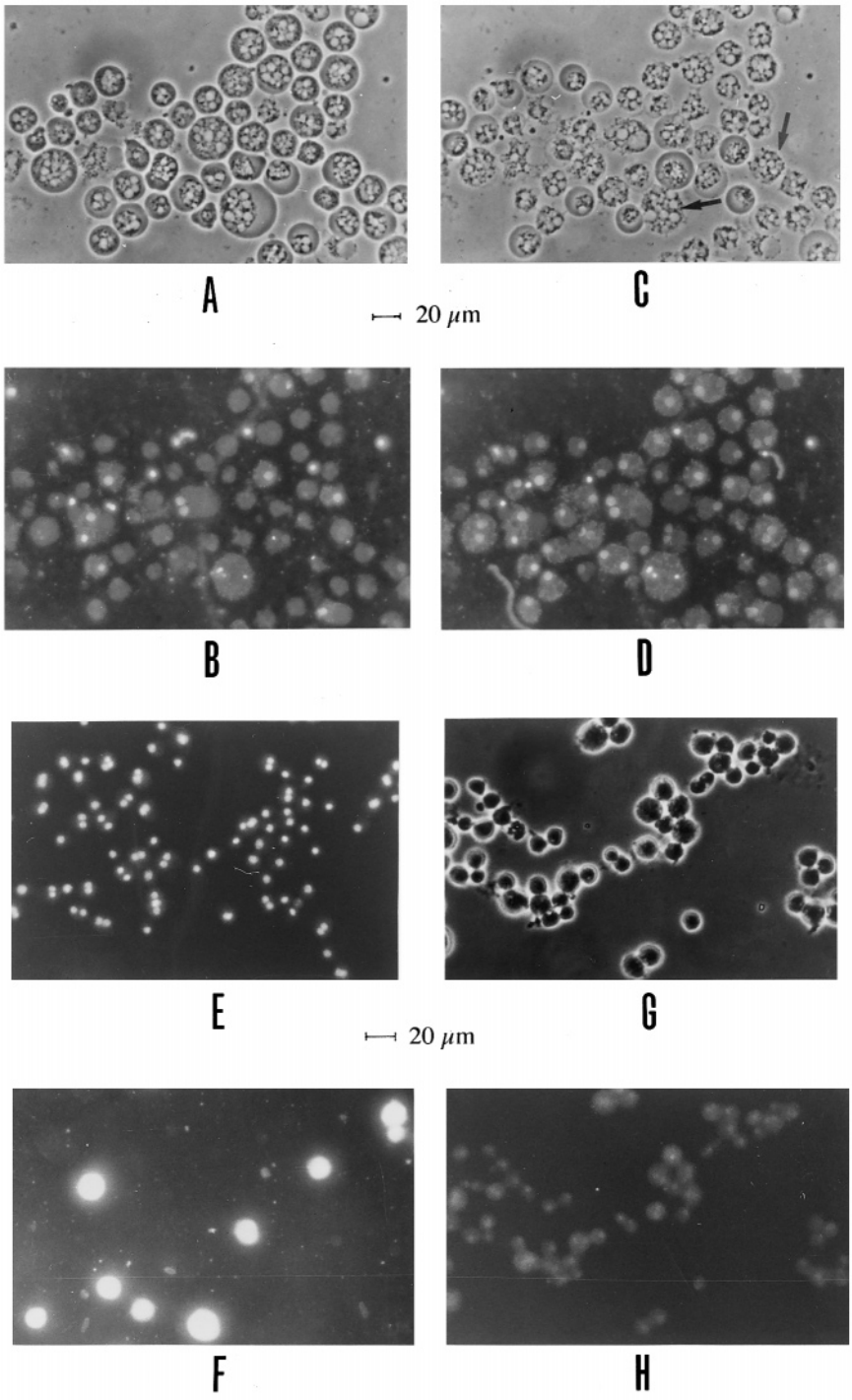

Figure 1. Light microscopy of *D. discoideum* cells after vital staining with HO342. (*A–D*): HO342 vitally stained live cells were observed by phase contrast (*A*) and UV fluorescence (*B*) after 7 h incubation at 4 °C; the same cells were observed about 10 min later (*C*, *D*). (*E–H*): Immediately after HO342 vital staining, cells were fixed either in methanol:buffer A (70:30 v/v) (*E*) or in 2.5% glutaraldehyde (*F*) and observed by UV fluorescence. Control cells without HO342 vital staining, fixed in 70% methanol, were observed by phase contrast (*G*) and UV fluorescence microscopy (*H*). Bars, 20 μm.

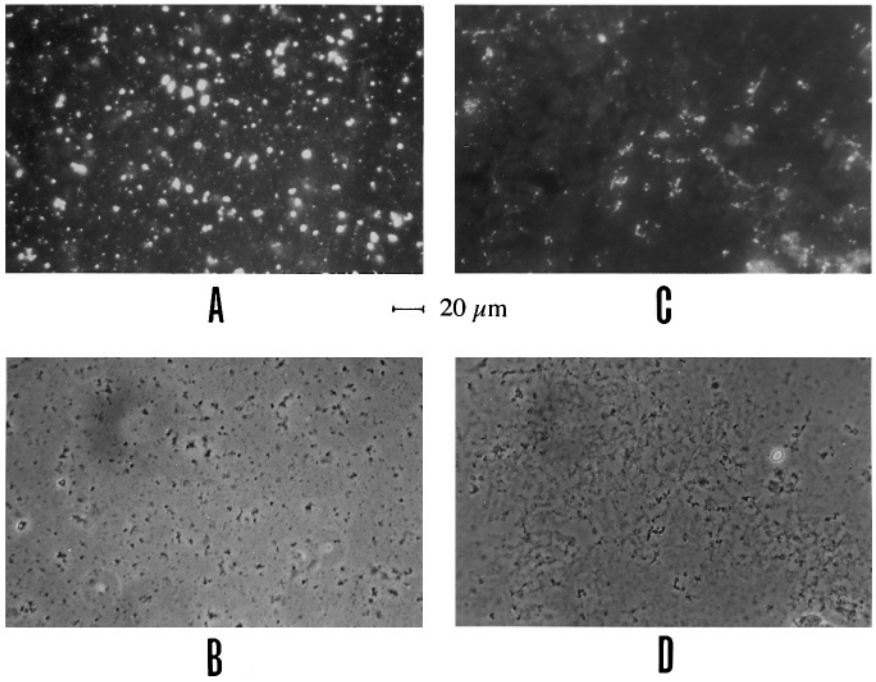

Figure 2. Light microscopy of concentrated extracellular fluorescent material from *D. discoideum* cells after vital staining with HO342. *Dd* extracellular material $\times 100$ concentrated (pelleted at 105,000*g*) (*A*, *B*) or $\times 10$ concentrated (pelleted at 20,000*g*) (*C*, *D*) was observed by UV fluorescence (*A*, *C*) and phase contrast microscopy (*B*, *D*). Bar, 20 μm.

for fixation-induced cell lysis, observation of unstained cells fixed in 70% methanol showed the absence of cell lysis (fig. 1G) and a faint autofluorescence distinct from the signals discussed above (fig. 1H). These data suggest that live *Dd* cells exhibit a strong constitutive nuclear resistance to HO342 staining, which decreases under progressive cold and oxygen stresses.

Extracellular fluorescent material was visible in a medium of HO342 vitally stained cells, either alive (fig. 1B, D) or post-fixed in 2.5% glutaraldehyde (fig. 1F). Such material was further evidenced by a 105,000*g* hundredfold concentration of the extracellular medium after HO342 vital staining of cells (see 'Materials and methods'). In these conditions, fluorescent structures were observed in the 105,000*g* pellet (fig. 2A, B), but were not detected in the supernatant. Since it was pelletable at 105,000*g*, the extracellular material was mostly particulate. A lower-speed tenfold concentration of the extracellular material at 20,000*g* for 1 h revealed fluorescent material (fig. 2C) which was more comparable in size to the punctuated material observed inside the cytoplasm of live cells (fig. 1B, D) or extracellularly (fig. 1B, D, F). This suggests that the concentration step may induce reorganization of the fluorescent extracellular material.

Similarly, extracellular material, concentrated from *Dd* cells grown without HO342, depicted a comparable morphological aspect by phase contrast microscopy but without any detectable fluorescence (data not shown).

Analysis by EM of *D. discoideum* extracellular material after HO342 vital staining. *Dd* extracellular material observed by EM at low magnification ($\times 11{,}500$) revealed numerous vesicular profiles of various sizes and shapes (fig. 3A). Some vesicles were rounded with 100–300 mm diameters (fig. $3B_1$, B_2). At higher magnification ($\times 73{,}000$), the electron-dense surface of these round organelles or granules showed a lipid-like bilayer membrane (fig. 3C). Such organelles were not detected in the 105,000*g* centrifuged HL5 medium alone, either in the supernatant or in the pellet.

***D. discoideum* extracellular material contains proteins.** Table 1 shows the protein content of various fractions obtained from two different *Dd* cell cultures. The first one, vitally stained with HO342, was treated as described in 'Materials and methods', to obtain vesicles (V) which were further purified on a D_2O-sucrose gradient. The protein content of the different gradient fractions shows that most of the material, i.e. the highest amount of proteins, was found in the pellet and was therefore denser than 1.210 g/cm^3. The second one, a

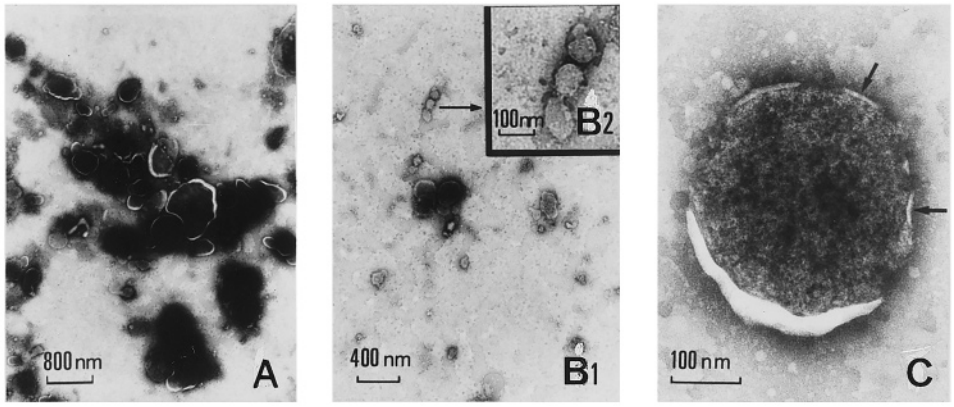

Figure 3. Electron microscopy of concentrated extracellular material from *D. discoideum* cells. Numerous vesicular profiles were observed by negative staining at low EM magnification (×11,500) (*A*), some with a rounded shape appearance (B_1, B_2). A lipid-like bilayer membrane (arrows) was visible at higher EM magnification (×73,000) (*C*).

Dd cell culture without vital staining, was treated to obtain the vesicular material (V′) and the clarified supernatant of culture medium after cell growth. The protein content of the vesicular material was compared with the protein content of cells present in the medium after growth and of the corresponding cell-free growth medium. A small amount of protein (about 1 mg) was found associated with the 105,000*g* centrifuged extracellular material from 100-ml cell-free growth medium, representing only about 4% of the growth medium proteins, and 1–1.5% of the total cell proteins present after 23 to 24 h growth. It is worth noting that the HL5 medium alone containing yeast extract, pelleted at 105,000*g*, exhibited a protein content comparable to the vesicular one.

Table 1. Protein content of the various fractions obtained from 100 ml of *D. discoideum* cell culture.

Sample	Proteins (mg)/100 ml medium
23-h HO342 (3 μg/ml) vitally stained *D. discoideum* cell culture	
700*g* pellet of 7×10^8 cells	64.1 ± 8.1
105,000*g* pellet of culture medium (V)	1.03 ± 0.11
D_2O-sucrose gradient fractions	
fraction loaded V	1.03 ± 0.11
fraction 1	0.17 ± 0.01
fraction 2	0.007 ± 0.001
fraction 3	0.012 ± 0.002
fraction 4	0.001 ± 0.002
fraction 5	0.058 ± 0.010
pellet P	0.42 ± 0.030
24-h *D. discoideum* cell culture	
700*g* pellet of 1.1 10^9	88.0 ± 16.0
700*g* cell-free supernatant (culture medium)	21.9 ± 5.4
105,000*g* supernatant of culture medium	21.1 ± 6.1
105,000*g* pellet of culture medium (V′)	0.91 ± 0.17
Control HL5 medium	
without centrifugation	24.3 ± 7.2
105,0000*g* supernatant (clarified medium)	24.0 ± 5.0
105,000*g* pellet (M)	1.03 ± 0.11

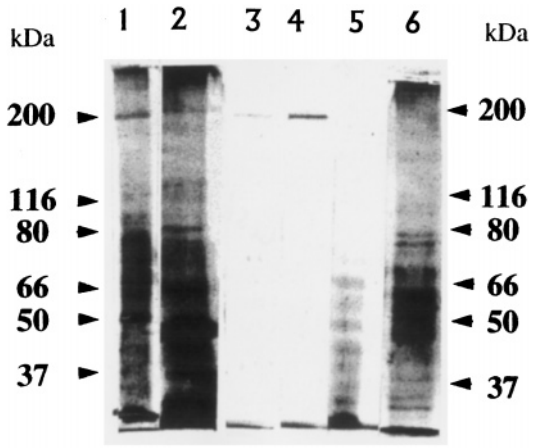

Figure 4. SDS-PAGE of concentrated extracellular material of *D. discoideum* cells. One to 10 μg of proteins were separated on 7% acrylamide SDS-PAGE, in sample buffer containing β-mercaptoethanol and 2 M urea. Silver staining was used for detection. Lane 1: 105,000*g* (×100) concentrated *Dd* extracellular material before loading on the gradient; lane 2: pellet of the D_2O-sucrose gradient (density from 1.050 to 1.210 g/cm^3); lane 3: fraction 3; lane 4: fraction 2; lane 5: fraction 1 of the gradient; lane 6: 105,000*g* (×100) concentrated pellet of HL5 culture medium alone.

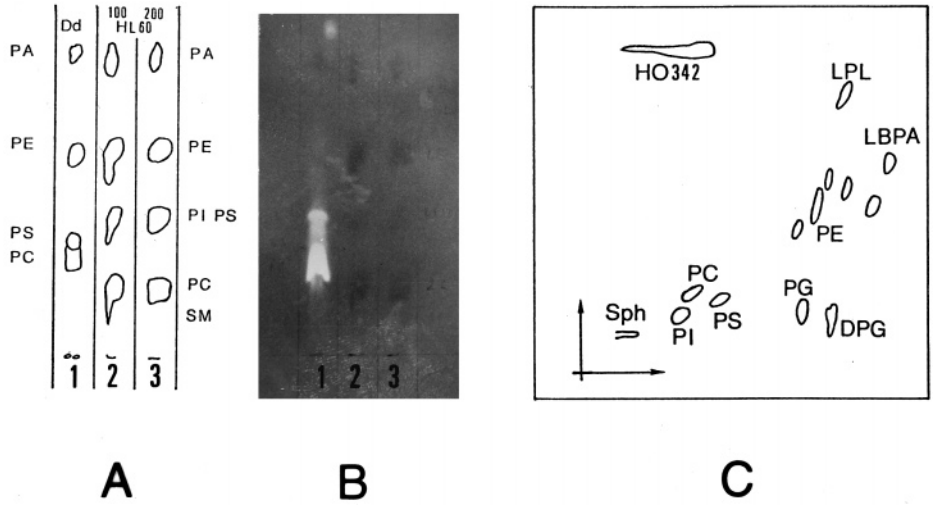

Figure 5. Identification by TLC of phospholipids in *D. discoideum* extracellular material. (*A*) Lane 1: one-dimensional TLC migration of phospholipids extracted from *Dd* extracellular material after HO342 vital staining of the cells; lanes 2 and 3: HL60 plasma membrane phospholipids at two concentrations. (*B*) Same TLC plate observed under UV light. (*C*) Two-dimensional TLC migration of phospholipids from *Dd* extracellular material, stained by iodide and ninhydrin. An HO342 fluorescent spot was also detectable when observed under UV light, but was clearly distinct from each phospholipid. PA, phosphatidic acid; PC, phosphatidylcholine; PE, phosphatidylethanolamine; PI, phosphatidylinositol; PS, phosphatidylserine; PG, phosphatidylglycerol; DPG, diphosphatidylglycerol; LPL, lysophosphatidic lipid; LBPA, lyso *bis*-phosphatidic acid; and Sph, sphingomyelin.

When analysed by SDS-PAGE (fig. 4), extracellular vesicles (V), prepared from HO342 vitally stained cells before the D_2O-sucrose gradient, exhibited numerous polypeptides with molecular mass between 35 and 200 kDa (lane 1). After gradient fractionation, the same components were found in the pellet (P) (lane 2). A 200-kDa polypeptide seemed to be characteristic of the vesicular material, since it was present in all vesicular fractions (lanes 1–4), but in fraction 1 (lane 5). The pattern of polypeptides originating from a control 105,000*g* pellet of the medium alone (lane 6) was more like to this lighter fraction of vesicles after gradient (lane 5), without a 200-kDa component. The D_2O-sucrose gradient appeared to separate, at least partially, the vesicular material from the medium material.

***D. discoideum* extracellular material contains phospholipids.** To confirm the lipid bilayer nature observed by EM (fig. 3C), a lipid extraction was performed from concentrated *Dd* extracellular material, purified from cells either vitally stained with HO342 or not. After HO342 vital staining of the cells, one-dimensional TLC (fig. 5A) revealed the presence of phospholipid species characteristic of cell membranes: PA and PE were easily identified by comparison with phospholipids originating from HL60 plasma membranes [13]. Two other spots possibly represent PI, PS and PC for which migration might have been slightly modified by HO342 comigration. Indeed, these two spots were fluorescent under UV light (fig. 5B). The presence of PC, PI, PS and PE was confirmed by two-dimensional TLC, performed on the same material (fig. 5C). PE and PS were double-stained by iodide and ninhydrin, specific for amino phospholipids. In addition, sphingomyelin (Sph), phosphatidylglycerol (PG), diphosphatidylglycerol (DPG) and some lysophosphatides were identified. These results are in crude agreement with the described phospholipid composition of *Dd* cell membranes [17], except for Sph and DPG, which were not identified. After two-dimensional TLC, HO342 migrated with a rate clearly different from that of each phospholipid, demonstrating the absence of actual HO342 binding to vesicle phospholipids. Without HO342 vital staining of the cells, phospholipids from concentrated extracellular material exhibited a comparable migration by TLC (data not shown).

Nucleic acids copurify with *D. discoideum* extracellular vesicles. Since HO342 is a specific marker of nucleic acids, we checked the presence of these components copurified with extracellular vesicles by 1% agarose gel electrophoresis. Experiments were performed on samples purified from 105,000*g* concentrated *Dd* extracellular vesicles, prepared from cells grown either with HO342 vital staining or without. In both cases, four main components appeared under UV excitation of ethidium bromide. As shown without HO342 vital staining (fig. 6), one component migrated with an apparent size higher than 21 kb (lane 2 or 6), relatively to

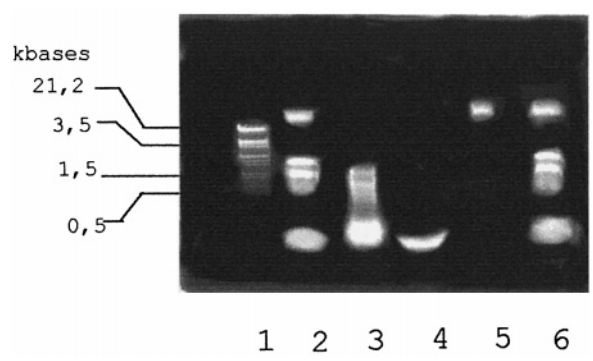

Figure 6. Agarose gel electrophoresis of nucleic acids purified from *D. discoideum* concentrated extracellular vesicles: identification of RNA. Lane 1: λ DNA markers [λ (*Hind*III, *Eco*RI)], with sizes ranging from 0.564 to 21.226 kb; lanes 2 and 6: nucleic acids purified from *Dd* vesicles; lane 3: control of HL5 medium without sustained cell growth, treated as the extracellular growth medium for nucleic acid extraction from *Dd* vesicles; lane 4: nucleic acids purified from total yeast extract, used for preparing HL5 growth medium, as a control; lane 5: nucleic acids purified from *Dd* vesicles, treated by 1 μg/ml of RNase (DNase free).

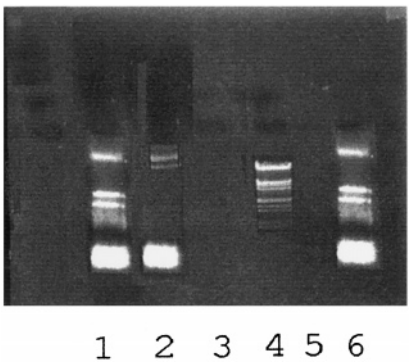

Figure 7. Agarose gel electrophoresis of nucleic acids purified from *D. discoideum* concentrated extracellular vesicles: identification of DNA. Lanes 1 and 6: nucleic acids purified from *Dd* vesicles; lanes 2 and 3: nucleic acids purified from *Dd* vesicles, treated with 1 U/ml of DNase (lane 2) and 4 U/ml of DNase (lane 3); lane 4: λ DNA markers [λ (*Hind*III, *Eco*RI)], with sizes ranging from 0.564 to 21.226 kb; lane 5: λ DNA markers [λ (HindIII, EcoRI)], treated with 1 U/ml of DNase.

λ DNA markers [λ (*Hind*III, *Eco*RI)] (lane 1). Some components migrated in the range of 3.5–1.5 kb, whereas a heavy front of degraded nucleic acids migrated below 0.5 kb. As a control, the 105,000*g* pellet of pure HL5 medium depicted three components, migrating below 3.5 kb (lane 3). A further control was performed on a hundredfold concentrated yeast extract, used at a concentration of 7 g/l for preparation of HL5 medium. This showed merely the heavy front of degraded nucleic acids (lane 4). Only nucleic acids purified from concentrated *Dd* extracellular vesicles exhibited the largest component of apparent size >21 kb. The lower size components could not actually be ascribed to *Dd* extracellular vesicles, since components migrating in about the same range were present in HL5 medium alone. To elucidate the nature of the observed nucleic acid bands, RNase and DNase digestion of the purified samples was performed prior to gel electrophoresis. By RNase (DNase-free) treatment (fig. 6), the three lower-size components, purified from *Dd* extracellular vesicles (lane 5) and from HL5 medium alone (data not shown), disappeared. They were, therefore, identified as RNA. On the contrary, the higher-size component characteristic of *Dd* extracellular vesicles, which remained after RNase treatment (lane 5), appeared not to be RNA. This was confirmed by DNase treatment of nucleic acids purified from *Dd* extracellular vesicles (fig. 7), showing that the higher-size component (lane 1 or 6) disappeared as a function of DNase concentration at 1 U/ml (lane 2) or 4 U/ml (lane 3). The λ DNA markers [λ (*Hind*III, *Eco*RI)] (lane 4) treated by 1 U/ml DNase are shown on lane 5 as a control. The characteristic *Dd* vesicle-copurifying nucleic acid species was, therefore, unambiguously identified as a DNA fragment with a size >21 kb. It is to be stressed that this extracellular DNA was detected independent of cell HO342 vital staining.

Since the extracellular vesicles were fluorescent under UV light after HO342 vital staining of the cells (fig. 2A, C), we looked to see whether the fluorescence originated from HO342 either free or DNA-bound. It has been shown [18] that, in bound condition, this A-T specific stain of double-stranded DNA depicts enhanced fluorescence with excitation and emission maxima at 352 nm and 465 nm, respectively. By comparison, the excitation and emission maxima of free HO342 fluorescence are 339 nm and 510 nm, respectively. As shown for uncorrected fluorescence spectra (fig. 8A), such a red-shift for excitation and a blue-shift for emission maxima of DNA-bound HO342 were observed (2), relative to fluorescence of free HO342 (3 μg/ml in buffer A) (1). *Dd* cells were freeze-thawed at -20 °C and stained after thawing with the same HO342 concentration. Such cell treatment prior to HO342 staining facilitates dye access to the nucleus without changing its solvent environment and allows a measure of the more A-T-specific bound DNA-HO342 contribution. Compared with the fluorescence of free HO342 peaking at 480 nm (1), the emission maximum was shifted to 460 nm with an intensity eight times higher (2) using the same 370-nm excitation wavelength. Emission and excitation spectra of control unstained freeze-thawed cells are given for comparison (3). As shown in the inset of figure 8B, after HO342 vital staining of *Dd* cells at a concentration of 12 μg/ml, live cells gave rise to a low-intensity emission

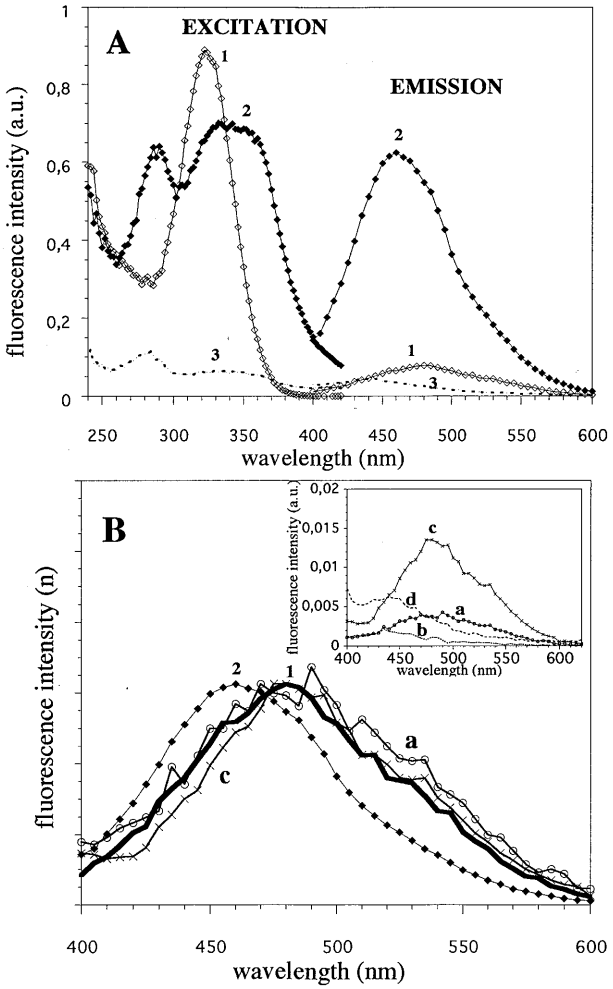

Figure 8. Spectral characteristics of HO342 emission from *D. discoideum* live cells and concentrated extracellular material after HO342 vital staining of the cells. (*A*) HO342 (3 μg/ml) was either free (1) or associated with previously −20 °C freeze-thawed *Dd* cells (2). Such cold treatment gave HO342 better nuclear access without changing the cell environment. Emission spectra were recorded at a fixed 370-nm excitation wavelength. Excitation spectra were recorded at a fixed 450-nm emission wavelength. The dotted line represents control of unstained −20°C freeze-thawed cells (3). (*B*) Fluorescence intensities normalized relatively to the intensity maximum of A-T-specific DNA-bound HO342 fluorescent emission (2). Free HO342 fluorescence (1); HO342 fluorescence from *Dd* live cells stained with 12 μg/ml of HO342 for 1 h (a); HO342 fluorescence from *Dd* concentrated extracellular material, prepared after 70 h vital staining of the cells with 63 μg/ml of HO342 (c). Inset represents the same spectra before normalization. Dotted lines represent control autofluorescence of live cells (b) and of concentrated extracellular material (d) without previous HO342 vital staining of the cells. Emission spectra were recorded at a fixed 365-nm excitation wavelength.

spectrum (a), as compared with control autofluorescence emission of unstained cells (b), both excited at the same 365-nm wavelength. With the same 365-nm excitation, a relatively low HO342 fluorescence emission was also observed for 20,000*g* tenfold concentrated extracellular material (c), prepared after (63 μg/ml) HO342 vital staining of the cells, as compared with autofluorescence of the extracellular material (d) prepared from control cells. Figure 8B shows normalization of the three emission spectra of either free HO342 (1) or live cells (a) and concentrated extracellular material (c) after HO342 vital staining of cells, relative to the intensity of the 460-nm emission peak of the DNA-bound HO342 spectrum (2). This normalization showed a predominant contribution of free HO342 to the spectra in both live cells (a) and concentrated extracellular material (c). In the extracellular vesicles, the presence of a minor fraction of HO342 bound to copurified DNA and contributing weakly to the observed emission fluorescence (c) cannot be excluded by this study.

Discussion

In the present work, we first observed by light microscopy that *Dd* cells vitally stained with HO342 released fluorescent material in their growth medium. After concentration and observation by EM, this material turned out to be organelles of about 100 to 300 nm in diameter, surrounded by what looked like a lipid bilayer envelope. The membranous nature of this envelope was confirmed by extraction and identification of the lipids from the concentrated extracellular material. We can therefore conclude that HO342 vitally stained *Dd* cells were releasing fluorescent vesicles in the extracellular medium. These vesicles were further analysed with regard to both their macromolecular content and their fluorescence properties. Some proteins were present on the electrophoretic pattern with mainly one 200-kDa polypeptide characteristic of the vesicles. No component around 170 kDa was detectable in the present experimental conditions. This corresponds to the molecular weight of the (P-gp) from *Dd* cells [6]. Since we have shown that this (P-gp) was nonfunctional [2], its presence in the vesicles was not further controlled by immunoblot.

A major DNA component of relatively high size (>21 kb) was found associated with the released vesicles, as shown by specific enzyme digestion followed by agarose electrophoresis. Fluorescence emission spectrum of the concentrated extracellular material evidenced a predominant contribution of the free HO342 monomer. However, the presence of a minor contribution of an A-T-specific DNA-HO342 complex could not be excluded. It is also possible that HO342 and DNA are present in different locations inside or around the vesicles, precluding mutual interaction.

It is worth emphasizing the presence of both extracellular vesicles and copurifying DNA in experiments carried

out on cells grown without any HO342. HO342 fluorescence has simply been a powerful tool for detecting the extracellular vesicles. It is noteworthy that the process of membrane microvesicle shedding appears to occur in many eukaryotic cell lines and is involved in synaptic transmission [19]. More recently, secretion of cellular microvesicles, not linked to programmed cell death, has been reported as a general cellular property [20–25]. This was observed in quite different studies dealing with activated cells [20, 21], virion infected cells [22–24] or adaptation to antibody-mediated injury [20, 25]. In the two more recent papers [23, 24], extracellular microvesicles from uninfected cells were prepared by methods comparable to ours. These vesicles depicted a size heterogeneity from 50 to 1000 nm in diameter. Moreover, cellular proteins, RNA and DNA were also found associated with the vesicles. As stressed by Glushankof et al. [23], the role of this vesiculation in normal cell function has yet to be defined.

***D. discoideum* extracellular vesicles as mediators of cell resistance against HO342 vital staining.** The primitive eukaryote *D. discoideum* has frequently been chosen in cell biology [26, 27], because each step of its life cycle – growth, aggregation, morphogenesis, differentiation, spore germination – is temporally distinct. This simple both in vitro and in vivo model has been used previously for fundamental studies concerning drug resistance [2]. In live *Dd* cells, we noticed that nuclei were poorly accessible to HO342 vital staining, the cytoplasm exhibiting a faint punctuated fluorescence pattern. The present data indicate that the observed cytoplasmic vesiculation and shedding of vesicles associated with HO342 contribute to the elimination of HO342. We suggest that what we have observed might be a new mechanism of eukaryotic cell resistance against penetration of the DNA-targeted vital dye in the nucleus.

The cellular resistance to cytotoxic drugs remains a major problem in cancer chemotherapy [5]. Due to its higher fluorescence quantum yield, compared with the clinically used anthracyclines, HO342 has been a drug of choice for in vitro measurements of cellular resistance to fluorescent cytotoxic drugs [28]. As shown here for *Dd*, the reduced nuclear binding of HO342 was correlated to drug resistance in murine cell lines [29]. The role of P-gp as the only protein involved in cell multidrug resistance is questioned by recent demonstrations of a number of other proteins contributing to the multidrug resistance phenotype (see ref. 30 for a review). Indeed, the present results are not in agreement with the use of HO342 as a functional test for measuring only P-gp activity [31].

Our interpretation of cytoplasmic vesiculation and shedding of vesicles associated with HO342 as part of a process of HO342 elimination might fit with the recently stressed importance of drug sequestration in multidrug resistance against other DNA-targeted drugs like anthracyclines [32–34]. It might also be related to the recent involvement of lung resistance protein (LRP) in non-P-gp multidrug resistance [35]. This protein, which is mainly located in vesicles but might have a nuclear-cytoplasmic transport function [36], has recently been identified as the human major vault protein [37]. Vaults, as new organelles in search of a function [38], might contribute to the cellular detoxification against structurally unrelated xenobiotics [39]. Since *Dd* cells are one of the two most abundant eukaryotic sources of vaults [40], it would be interesting to clarify the link of *Dd* extracellular vesicles with vaults.

Inasmuch as the *Dd* vesicles were evidenced in the extracellular medium without any chemical stress, their role cannot be limited to a cell defence process, as discussed below.

***D. discoideum* extracellular vesicles as DNA transporters.** *Dd* extracellular vesicles might be more generally involved in the process of DNA transport and function as intercellular communication mediators. Our observations might be relevant not only to the process of cellular shedding of vesicles [19–25], but also to the reported excretion of DNA [41–43].

The recent unravelling of cellular suicide as programmed cell death (PCD) [44] might explain the presence of DNA in extracellular fluids during differentiation and development, or following a strong cell aggression like transfection or cancer. In the case of *Dd* cells, PCD has not been observed during exponential cell growth, but it has been claimed as being induced during development [45]. Moreover, even in this induced PCD, neither small (200 bp) nor large DNA fragments (i.e. 50–300 kb) were observed. As shown here, we did observe a high molecular weight DNA fragment associated with the extracellular vesicles during exponential cell growth. This occurred without any detectable loss of cell viability. Therefore, our observation seems unrelated to the reported *Dictyostelium* PCD. It is more likely related to the high molecular weight fragmentation of DNA in normal murine thymocytes. In the absence of apoptotic inducers, such a process has been ascribed to an unknown physiological function [46].

Conclusion

The present observation of a cellular traffic targeting HO342 into the extracellular medium by means of vesicles indicates a new possible mechanism for the high cellular resistance of *Dd* cells against this DNA-

targeted vital stain. However, before being able to extend such a mechanism mediated by vesicular traffic to detoxification of other xenobiotics, experiments should be carried out with anthracyclines and other cytotoxic drugs binding to targets other than nucleic acids.

The presence of these extracellular vesicles without any chemical stress strongly suggests a more general intercellular function for these new organelles, as recently suggested for similar vesicles shed from normal mammalian cells.

Acknowledgements. We thank G. Tham for her skillful technical assistance with *Dictyostelium* cells and for the preparation of figures. J.-M. Lepecq is acknowledged for his photographic work. This research was performed, in part, at the Institut Curie, Section de Physique et Chimie and partially presented, in an abstract form, to the International *Dictyostelium* Meeting, June 1995, Dourdan, France.

1 Tatischeff I., Lavialle F., de Paillerets C., Weintraub H., Tham G. and Alfsen A. (1993) Carcinogenic benzo(a)pyrene and non-carcinogenic benzo(e)pyrene discriminated by *Dictyostelium discoideum* cells through internalization In: Polycyclic Aromatic Compounds, PAH XIII (supplement to vol. 3 of the journal), pp. 695–702, Garrigues P. and Lamotte M. (eds), Gordon and Breach Science Publishers, Switzerland

2 Tatischeff I., Lizard G., Roignot P. and Lavialle F. (1993) *Dictyostelium discoideum*, a new eukaryotic model for analyzing cell resistance. Biol. Cell **79:** 9a

3 Bradley G., Juranka P. F. and Ling V. (1988) Mechanism of multidrug resistance. Biochim. Biophys. Acta **948:** 87–128

4 Endicott J. A. and Ling V. (1989) The biochemistry of P-glycoprotein-mediated multidrug resistance. Annu. Rev. Biochem. **58:** 137–171

5 Gottesman M. M. and Pastan I. (1993) Biochemistry of multidrug resistance mediated by the multidrug transporter. Annu. Rev. Biochem. **62:** 385–427

6 Tatischeff I. and Lavialle F. (1993) Immunological evidence of a P-glycoprotein in the microorganism *Dictyostelium*. C. R. Acad. Sci. Paris **316:** 560–563

7 Loomis W. F. (1975) *Dictyostelium discoideum*: A Developmental System, Academic Press, New York

8 Watts D. J. and Ashworth J. M. (1970) Growth of myxamoebae of the cellular slime mould *Dictyostelium* in axenic culture. Biochem. J. **119:** 171–174

9 Bomsel M., de Paillerets C., Weintraub H. and Alfsen A. (1988) Biochemical and functional characterization of three types of coated vesicles in bovine adrenocortical cells: implication in the intracellular traffic. Biochemistry **27:** 6806–6813

10 Peterson G. L. (1977) A simplification of the protein assay method of Lowry et al. which is more generally applicable. Anal. Biochem. **83:** 346–356

11 Laemmli V. K. (1970) Cleavage of structural proteins during the assembly of the head of bacteriophage T_4. Nature **227:** 680–685

12 Folch J., Lees M. and Sloane-Stanley G. H. (1957) A simple method for the isolation and purification of total lipids from animal tissues. J. Biol. Chem. **226:** 497–509

13 Geny B. and Cockcroft S. (1992) Synergistic activation of phospholipase D by protein kinase C- and G-protein-mediated pathway in streptolysin O-permeabilized HL60 cells. Biochem. J. **284:** 531–538

14 Rouser G., Fleisher S. and Yamamoto A. (1970) Two dimensional thin layer chromatographic separation of polar lipids by phosphorus analysis of spots. Lipids **5:** 494–496

15 Sambrook J., Fritsch E. F. and Maniatis T. (1989) Molecular Cloning: A Laboratory Manual, 2nd ed., Cold Spring Harbor Laboratory Press, Cold Spring Harbor, NY

16 Thiery R. (1989) Etudes biophysiques sur la croissance, l'agrégation et les signaux intercellulaires chez *Dictyostelium discoideum*, PhD thesis, University of Paris 6

17 Murray B. A. (1982) Membranes. In: The Development of *Dictyostelium discoideum*, pp. 71–116, Loomis W. F. (ed.), Academic Press, New York

18 Arndt-Jovin D. J. and Jovin T. M. (1989) Fluorescence labeling and microscopy of DNA. In: Methods in Cell Biology, vol. 30, Fluorescence of Living Cells in Culture, part B, pp. 417–448, Lansing Taylor D. and Wang Y.-L. (eds), Academic Press, San Diego

19 Trams E. G., Lauter C. J., Salem N. Jr. and Heine U. (1981) Exfoliation of membrane ecto-enzymes in the form of microvesicles. Biochim. Biophys. Acta **645:** 63–70

20 Raposo G., Nijman H. W., Stoorvogel W., Leijendekker R., Harding C. V., Melief C. J. M. et al. (1996) B lymphocytes secrete antigen-presenting vesicles. J. Exp. Med. **183:** 1161–1172

21 Fourcade O., Simon M. F., Viodé C., Rugani N., Leballe F., Ragab A. et al. (1995) Secretory phospholipase A_2 generates the novel lipid mediator lysophosphatidic acid in membrane microvesicles shed from activated cells. Cell **80:** 919–927

22 Ott D., Coren L. V., Kane B. P., Busch L. K., Johnson D. G., Sowder II R. C. et al. (1996) Cytoskeletal proteins inside human immunodeficiency virus type 1 virions. J. Virol. **70:** 7734–7743

23 Gluschankof P., Mondor I., Gelderblom H. R. and Sattentau Q. J. (1997) Cell membrane vesicles are a major contaminant of gradient-enriched human immunodeficiency virus type-1 preparations. Virology **230:** 125–133

24 Bess J. W. Jr, Gorelick R. J., Bosche W. J., Henderson L. E. and Arthur L. O. (1997) Microvesicles are a source of contaminating cellular proteins found in purified HIV-1 preparations. Virology **230:** 134–144

25 Yusawa Y., Brett J., Fukatsu A., Matsuo S., Caldwell P. R. B., Niesen N. et al. (1995) Interaction of antibody with Forssman antigen in guinea pigs. A mechanism of adaptation to antibody- and complement-mediated injury. Am. J. Pathol. **146:** 1260–1272

26 Loomis W. F. (1982) The Development of *Dictyostelium discoideum*, Academic Press, New York

27 Spudich J. A. (1987) *Dictyostelium discoideum*: molecular approaches to cell biology. Methods in Cell Biology, vol. 28, Academic Press, New York

28 Lahmy S., Salmon J. M., Vigo J. and Viallet P. (1992) Identification of multidrug resistant cells in sensitive Friend leukemia cells by quantitative videomicrofluorimetry. Cell Biochem. Funct. **10:** 9–17

29 Morgan S. A., Watson J. V., Twentyman P. R. and Smith P. J. (1990) Reduced nuclear binding of a DNA minor groove ligand (Hoechst 33342) and its impact on cytotoxicity in drug resistant murine cell lines. Br. J. Cancer **62:** 959–965

30 Baggetto L. G. (1997) Non-P-glycoprotein novel proteins involved in human cancer multidrug resistance. Bull. Cancer **84:** 385–390

31 Lizard G., Maynadié M., Roignot P., Lizard-Nacol S. and Poupon M. F. (1995) Evaluation of multidrug resistant phenotype by flow cytometry with monoclonal antibodies and functional tests. Bull. Cancer **82:** 211–217

32 Slapak C. A., Lecerf J. M., Daniel J. C. and Levy S. B. (1992) Energy-dependent accumulation of daunorubicin into subcellular compartments of human leukemia cells and cytoplasts. J. Biol. Chem. **267:** 10638–10644

33 Sognier M. A., Zhang Y., Eberle R. L., Sweet K. M., Altenberg G. A. and Belli J. A. (1994) Sequestration of doxorubicin in vesicles in a multidrug-resistant cell line (LZ-100). Biochem. Pharmacol. **48:** 391–401

34 Seidel A., Hasmann M., Löser R., Bunge A., Schaefer B., Herzig I. et al. (1995) Intracellular localization, vesicular accumulation and kinetics of daunorubicin in sensitive and multidrug-resistant gastric carcinoma EPG85-257 cells. Virchows Arch. **426:** 249–256

35 Scheper R. J., Broxterman H. J., Scheffer G. L., Kaaijk P., Dalton W. S., Vanheijningen T. H. M. et al. (1993) Overexpression of a M(r) 110,000 vesicular protein in non-P-glycoprotein-mediated multidrug resistance. Cancer Res. **53:** 1475–1479
36 Chugani D. C., Rome L. H. and Kedersha N. L. (1991) Evidence that vault ribonucleoprotein organelles dock at the nuclear pore complex. J. Cell Biol. **115:** 458a
37 Scheffer G. L., Wijngaard P. L. J., Flens M. J., Izquierdo M. A., Slovak M. L., Pinedo H. M. et al. (1995) The drug resistance-related protein LRP is the human major vault protein. Nature Med. **1:** 578–582
38 Rome L., Kedersha N. and Chugani D. (1991) Unlocking vaults: organelles in search of a function. Trends Cell Biol. **1:** 47–50
39 Izquierdo M. A., Scheffer G. L., Flens M. J., Schroeijers A. B., Vandervalk P. and Scheper R. J. (1996) Major vault protein LRP-related multidrug resistance. Eur. J. Cancer **32A:** 979–984
40 Kedersha N. L., Heuser J. E., Chugani D. C. and Rome L. H. (1991) Vaults. III. Vault ribonucleoprotein particles open into flower-like structures with octogonal symmetry. J. Cell Biol. **112:** 225–235
41 Anker P., Lyautey J., Lefort F., Lederrey C. and Stroun M. (1994) Transformation of NIH/3T3 cells and SW480 cells displaying a K-ras mutation. C. R. Acad. Sci. Paris **317:** 869–874
42 Chen X. Q., Stroun M., Magnenat J. L., Nicod L. P., Kurt A. M., Lyautey J. et al. (1996) Microsatellite alterations in plasma DNA of small cell lung cancer patients. Nature Med. **2:** 1033–1035
43 Nawroz H., Koch W., Anker P., Stroun M. and Sidransky D. (1996) Microsatellite alterations in serum DNA of head and neck cancer patients. Nature Med. **2:** 1035–1037
44 Steller H. (1995) Mechanisms and genes of cellular suicide. Science **267:** 1445–1449
45 Cornillon S., Foa C., Davoust J., Buonavista N., Gross J. D. and Golstein P. (1994) Programmed cell death in *Dictyostelium*. J. Cell Sci. **107:** 2691–2704
46 Solovyan V. T., Andreev I. Q., Kolotova T. Y., Pogribniy P. V., Tarnavsky D. T. and Kunakh V. A. (1997) The cleavage of nuclear DNA into high molecular weight DNA fragments occurs not only during apoptosis but also accompanies changes in functional activity of the nonapoptotic cells. Exp. Cell Res. **235:** 130–137